THE RECURSIVE STACKING OPERATOR (RSO) PART 2: APPLICATION TO HETEROGENEOUS MEDIA

B. Schwarz, C. Vanelle, and D. Gajewski

email: *benjamin.schwarz@zmaw.de*

keywords: *traveltimes, stacking, CRS, diffractions*

ABSTRACT

Multi-parameter stacking is an important tool to get a first reliable time image of the subsurface. The quality of this image and the respective parameter estimates heavily rely on the accuracy of the traveltime moveout description. The hyperbolic CRS operator reduces to the NMO hyperbola in the CMP gather. Hyperbolic moveout with offset, though, does not account for the curvature of the reflecting interface. The recursive stacking operator (RSO) is an implicit double-square-root expression of the traveltime and based on the assumption of a locally spherical reflector. We apply two different parameterizations of this operator in terms of the CRS attributes to synthetic datasets. For the simple case of a spherical reflecting interface in a constant vertical velocity gradient medium, application of RSO results in higher semblance values and more reliable attribute estimates than CRS and planar multifocusing over the full range of reflector curvatures, which in consequence leads to an improved approximate attribute-based poststack time migration. Comparison of the stack and migration results to the ones of CRS for the Sigsbee 2a model confirms the overall superior performance of RSO for a more realistic and complex subsurface setting.

INTRODUCTION

Stacking plays a crucial role in seismic reflection data processing. The common reflection surface (CRS) stack (Müller, 1999) is an extension of the classical CMP method in which summation is carried out not only in offset but also in midpoint direction. The result is an improved stacked section with a higher signal-to-noise ratio. The CRS traveltime operator is a surface of second order and equivalent to the NMO hyperbola in the CMP gather, which is only exact for a planar reflector in a constant velocity medium.

For the more general model of a spherical reflector, Vanelle et al. (2010) derived an implicit nonhyperbolic expression for the traveltime. Since this operator is applicable in a recursive fashion, it is called the recursive stacking operator (RSO). It is parameterized in terms of three attributes and the overburden velocity, which represent real subsurface properties for the homogeneous case. Since, however, this operator was derived under the assumption of a homogeneous overburden, the parameters lose their physical meaning if heterogeneity is present. The CRS parameters, in contrast, are surface-related quantities and thus, also valid in heterogeneous media. Schwarz et al. (2011) have introduced two different transformations from RSO to CRS parameters. While one of them is based on concepts of geometrical optics and incorporates the application of a time shift (from here on referred to as shifted RSO), the other is the result of a Taylor series expansion of the squared RSO traveltime (Taylor RSO).

The main goal of this work is to verify whether the promising results of the accuracy studies by Schwarz et al. (2011) can be confirmed for the actual stack. In the first part of our investigations the underlying model features a spherical reflector with a constant vertical velocity gradient overburden. For this medium, the attribute values can be forward calculated (see, e.g., Vanelle, 2002), which allows for a quantitative

evaluation of the estimates. In addition, we apply an approximate poststack time migration (Mann, 2002) to the stack, which directly uses the attributes. In the second part, the operators are applied to the Sigsbee 2a dataset, whose underlying model simulates a complex geological setting. We demonstrate that the application of Taylor RSO not only leads to higher semblance values and consequently an improved stacked section, but also to more reliable attribute estimates than the other methods, which clearly affects subsequent processing steps like the considered poststack time migration.

Schwarz et al. (2011) found that for a gradient in the overburden an iterative application of the RSO angle update does not lead to an increase in accuracy after the first step. Accordingly, for both RSO representations we will also use a single iteration during optimization and stack. All stacks, semblance and attribute values in this work are gained with the extended CRS implementation by Mann (2002). They represent the results of the final optimization, in which all three parameters are determined simultaneously. The starting values are the same for all operators and result from the extended pragmatic search strategy.

SPHERICAL REFLECTOR IN A GRADIENT MEDIUM

The simple model of a spherical reflector below a constant vertical velocity gradient overburden allows for the forward calculation of the kinematic attributes. With these, the quality of the individual operator's estimates of α, R_{NIP}, and R_N gained in the stacking procedure can be evaluated quantitatively. By prescribing the radius of the sphere, R, we are able to investigate the impact of reflector curvature on the accuracy of each operator. The stack is applied for four different radii from R =10 m, representing the limiting diffraction case to R =10000 m, i.e. a nearly planar interface. The vertical depth of the top of the reflector is kept constant at 1000 m. Since we deal with constant vertical velocity gradient media, analytical ray tracing is applied for the generation of the datasets. We investigate the case of constant velocity, with v_0 =2 km/s and a linear vertical velocity gradient in the overburden, $v(z) = v_0 + \gamma z$, with γ =1/s. Although the gradient can be considered unrealistically strong, it helps to judge the performance of each operator under extreme conditions.

For all investigations we have chosen a maximum offset of 2000 m, i.e. a maximum offset-over-depth-ratio of two. The horizontal midpoint displacements from the centre of the sphere, $x_m - x_c$, range from -2000 m to 2000 m. Due to the symmetry of the problem, only the midpoints between $x_m - x_c$ =0 and $x_m - x_c$ =2000 m are considered for illustration and comparison. The datasets consist of 401 CMP gathers each containing 81 traces. To simulate a more realistic scenario, Gaussian noise with a signal-to-noise ratio of 5 is added to the data. While all offsets are considered, the midpoint aperture is kept constant at 500 m for the optimization.

Semblance

The stacked sections resulting from the application of CRS, planar MF, shifted RSO, and Taylor RSO show (if at all) only minor differences in the waveforms. The main deviations merely constitute in lower or higher amplitudes of the stacked traces. In consequence, we will only discuss the respective semblance sections. Figures 1 and 2 show the semblance value as a function of $x_m - x_c$ for constant velocity and γ =1/s, respectively. Displayed are the graphs of the four operators for all four considered curvatures.

For constant velocity, CRS, due to its hyperbolicity in offset direction, provides a considerably poorer fit than the three double-square-root-based stacking operators when events stem from highly-curved interfaces. The semblance values of the two RSO parameterizations and planar MF are almost identical for all curvatures. For CRS, they are considerably fluctuating in regions of poor fit, whereas for the other three descriptions they show a smoother behavior with $x_m - x_c$.

CRS performs equally well in the gradient case and thus reveals a certain robustness with respect to velocity changes in the overburden. Like for constant velocity, the respective semblance values are lower for higher curvatures. The quality of fit of planar MF and shifted RSO noticeably decreases for higher horizontal displacements from the center of the sphere, when there is a velocity gradient in the overburden. The application of both operators results in significantly lower values of semblance, compared to the constant velocity case. Although this trend is, in principle, also noticeable for Taylor RSO, the differences are very small in general. The Taylor RSO operator maintains its superior fit over the full range

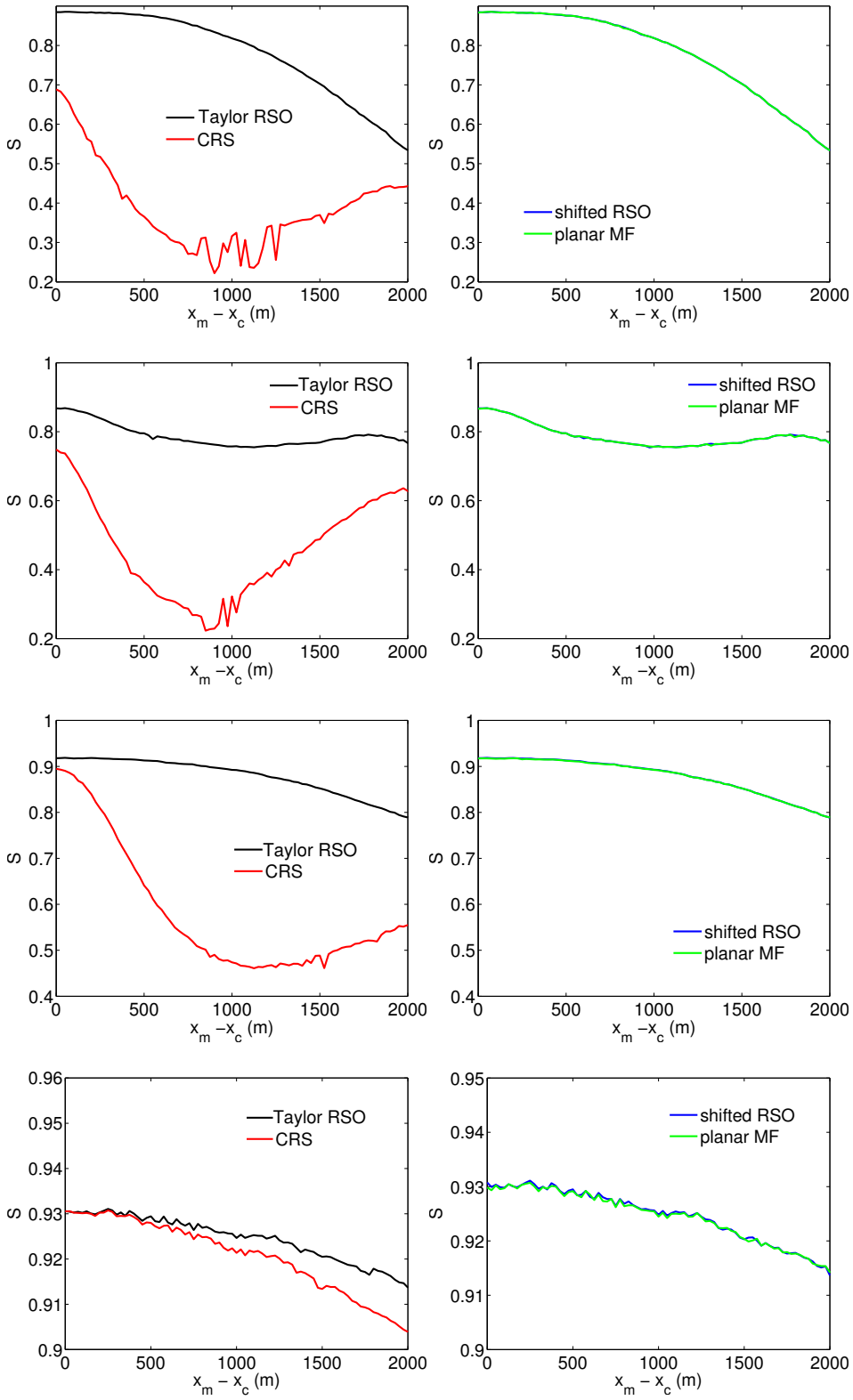

Figure 1: Semblance S as a function of the horizontal midpoint displacement $x_m - x_c$ for $R = 10$ m (top), $R = 100$ m (second row), $R = 1000$ m (third row), and $R = 10000$ m (bottom) and constant velocity. While the application of the three double-square-root-based descriptions leads to high semblance values, CRS rather poorly fits events in the prestack data when they stem from highly curved interfaces.

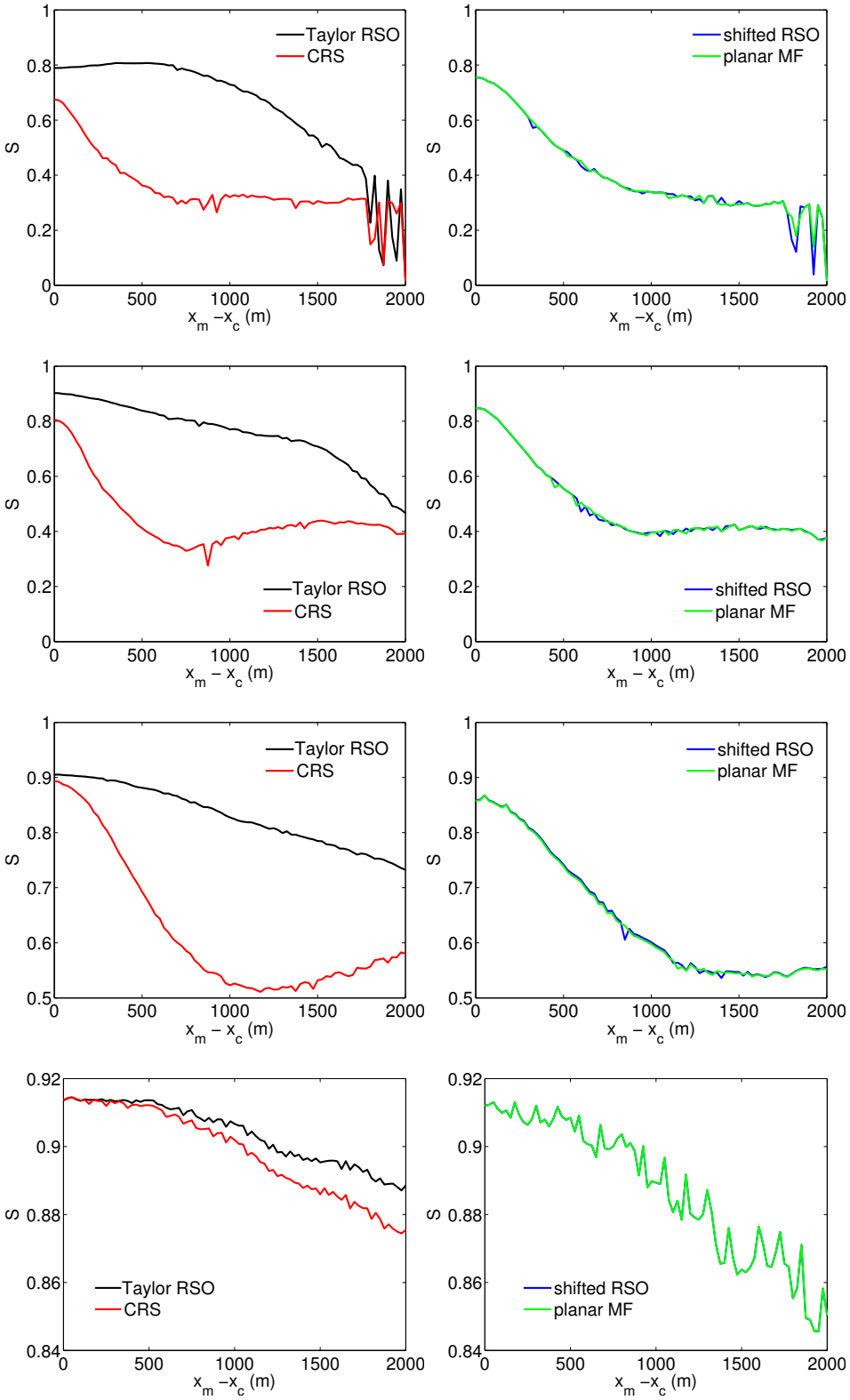

Figure 2: Semblance S as a function of the horizontal midpoint displacement $x_m - x_c$ for R =10 m (top), R =100 m (second row), R =1000 m (third row), and R =10000 m (bottom) and γ =1/s. While CRS overall maintains the performance of the constant velocity case, the semblance values of planar MF and shifted RSO are considerably smaller, when there is a gradient in the overburden. Taylor RSO still provides the best fit for all curvatures.

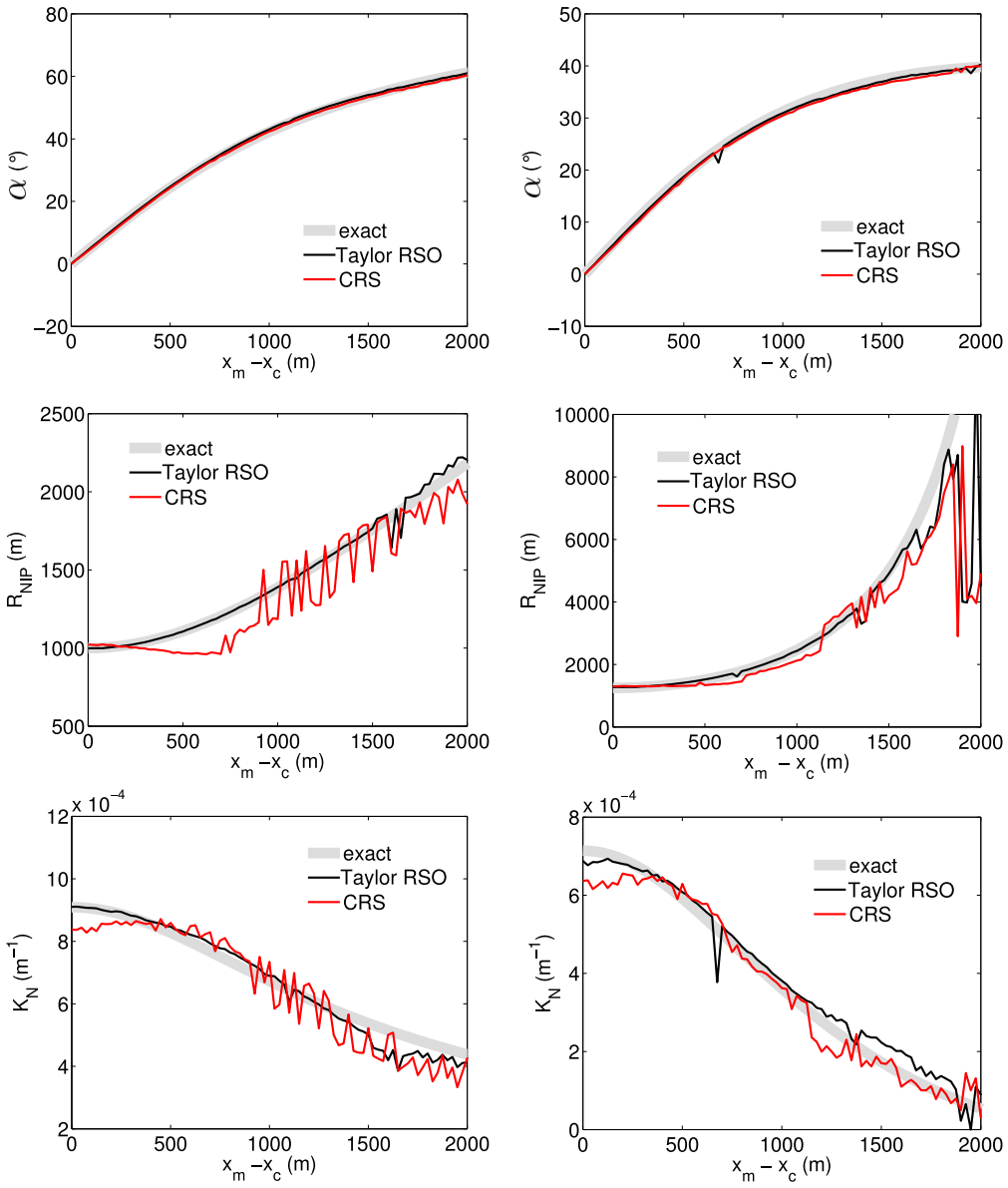

Figure 3: Attribute graphs for R =100 m for constant velocity (left) and γ =1/s (right). CRS systematically underestimates α and R_{NIP}, whereas R_N is overestimated. Taylor RSO overall provides the most reliable and consistent values for all three attributes.

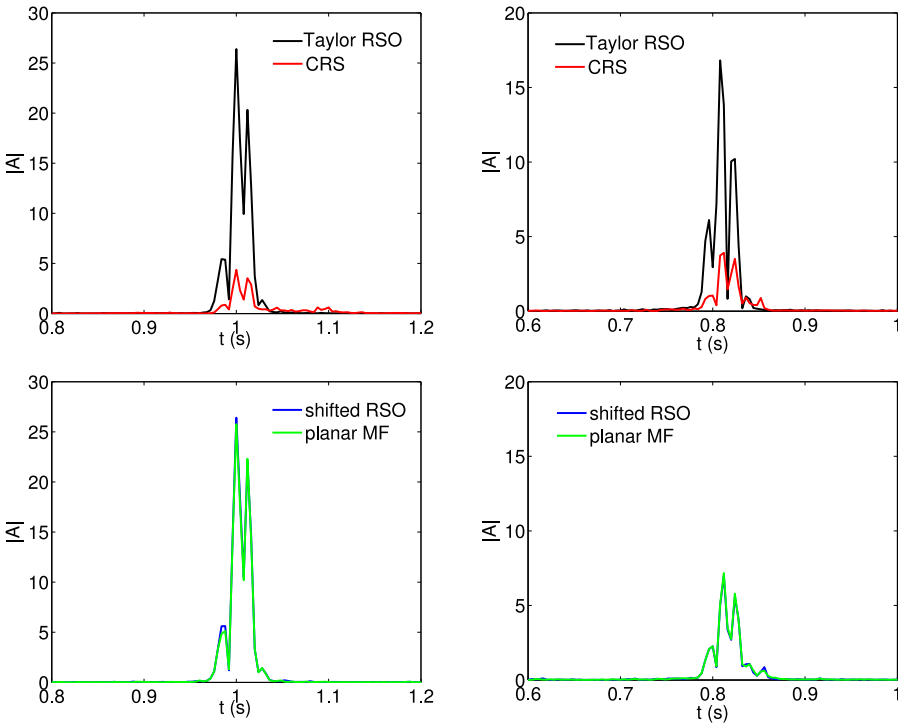

Figure 4: Absolute stacked amplitudes resulting from the application of the attribute-based poststack time migration for R =10 m for constant velocity (left) and γ =1/s (right). Displayed is the trace with $x_m = x_c$ only. While CRS manages to reproduce the results of the constant velocity case, the migrated amplitudes of planar MF and shifted RSO are considerably lower for heterogeneity. Taylor RSO provides a superior focusing of diffracted energy for both models. Please note the different scales.

of midpoint displacements and reflector curvatures.

As stated in the introduction, CRS is expected to perform best for a planar reflector. Indeed, its semblance values approach the ones of planar MF, shifted RSO, and Taylor RSO for R =10000 m. For the gradient overburden, CRS in this case even provides a better fit than planar MF and shifted RSO over the full investigated range of $x_m - x_c$.

Attributes

In Figure 3 the parameter graphs for R =100 m for constant velocity and γ =1/s are displayed. For homogeneous as well as for heterogeneous overburden, α, R_{NIP} and $K_N = 1/R_N$ are underestimated by the CRS operator. The respective values for the radii of the normal wave and the NIP-wave oscillate around the reference, whereas up to $x_m - x_c \approx$1600 m they are smooth functions of the displacement from the center of the sphere for Taylor RSO. For both models, the Taylor RSO parameter values are closest to the reference. The systematic underestimation of α, R_{NIP}, and R_N by the CRS operator shows even more clearly for the diffraction-like case of R =10 m. Although not displayed here, CRS and Taylor RSO behave similarly for the remaining values of R (Schwarz, 2011). The application of planar MF and shifted RSO leads to almost the same parameter values for the full range of $x_m - x_c$ and all reflector radii. The respective parameter graphs for planar MF and shifted RSO can be found in Schwarz (2011).

Figure 4 shows the absolute values of the stacked amplitudes resulting from the application of an attribute-based poststack time migration (Mann, 2002) to the datasets with R =10 m. This approximate Kirchhoff-type time migration aims to collapse the diffractions in the stack to their respective apex locations in midpoint and time. The parameters estimated by the double-square-root-based operators lead to a considerably higher amplitude and in consequence an improved migration result, compared to the ones

gained by the hyperbolic expression, i.e. CRS. While the CRS results are reasonable for heterogeneity, the ones of planar MF and shifted RSO become worse when there is a gradient in the overburden. The consistently high summed amplitude values of Taylor RSO, although in principle displaying the same trend as planar MF and shifted RSO, reflect the superior quality of attributes and stack.

SIGSBEE 2A

In order to investigate a complex subsurface setting, the Sigsbee 2a dataset was chosen, whose underlying model is dominated by a homogeneous salt body. Since Taylor RSO consistently showed the best performance for the generic examples of a spherical reflector and planar MF happens to almost coincide with the time-shift-based parameterization for all tested scenarios, we will from now on focus on the comparison of CRS and Taylor RSO. The latter operator is consequently denoted by 'RSO' only. In Schwarz (2011), the Sigsbee 2a results for planar MF and shifted RSO are displayed and discussed in detail. To ensure comparability with preceding results for this dataset, all stacking and optimization parameters are chosen according to Mann (2002).

Semblance and stack

Figure 5 shows the semblance sections resulting from the application of CRS and RSO, respectively. Both operators similarly approximate the response from the mostly unperturbed smoothly curved sediment-like strata above the top-of-salt. Moreover, events connected with discontinuities left of the salt body are equivalently described by both operators. Observe that the main deviation in semblance can be addressed to the very steep flanks of various diffraction patterns, stemming either from the highly curved features of the rugged top-of-salt or from the two horizons of equally spaced point diffractors. While CRS only provides a sufficient description in a very small vicinity of the diffraction's apex, application of RSO leads to high semblance values even for very large horizontal displacements. In particular, diffractions from the top-of-salt are poorly described by the hyperbolic CRS operator, whereas RSO provides a superior fit. To emphasize and support this finding, we refer to Figure 6, where the difference in semblance $\Delta S = S_{RSO} - S_{CRS}$ is displayed. Almost all diffraction events in the section are considerably better described by RSO. Even for events that stem from diffracting structures located in the deeper parts of the model, RSO provides a noticeably improved fit (see for example the inclined event at CMP number $\sim$400 and $t \approx$10 s). It is important to note the scale at this point. For almost all diffraction events, application of RSO leads to an increase in semblance of at least 0.2 up to 0.6, compared to CRS, meaning that large portions of most diffraction events in the data are described twice as well by the recursive approach.

The findings for the semblance section also apply to the actual stack. In Figure 7 and 8 the respective sections for CRS and RSO are displayed. The quality of the stacked section is equally good for nearly planar reflectors in the model. Especially for diffraction events however, application of RSO leads to noticeably higher amplitudes than CRS. The three red boxes indicate some of the most prominent differences between the CRS and the RSO stack. On the left and in the central box the steep flanks of the diffractions not only have higher amplitudes for RSO, they also show less distortions in the stacked waveform than the respective counterparts in the CRS-stacked section. Especially in the left and in the right box the amplitudes for RSO are considerably higher than the ones for CRS. The significantly better fit of the recursive approach to diffraction events in the prestack data not only leads to higher values of semblance, but also to an improved simulated zero-offset section.

Attributes

Figures 9 and 10 show the time-migrated CRS- and RSO-stacked section. The attribute estimates of both operators, in principle, allow for a significant focusing of diffracted energy. However, observe that diffraction events in the CRS-stacked section are overall not optimally collapsed for the top-of-salt. Application of RSO results in significantly less residuals of scattered energy in the time-migrated stacked section. The red boxes indicate portions of the section where the RSO stack leads to a superior attribute-based time-migrated result. While the top-of-salt shows discontinuities in the time-migrated CRS stack, for large

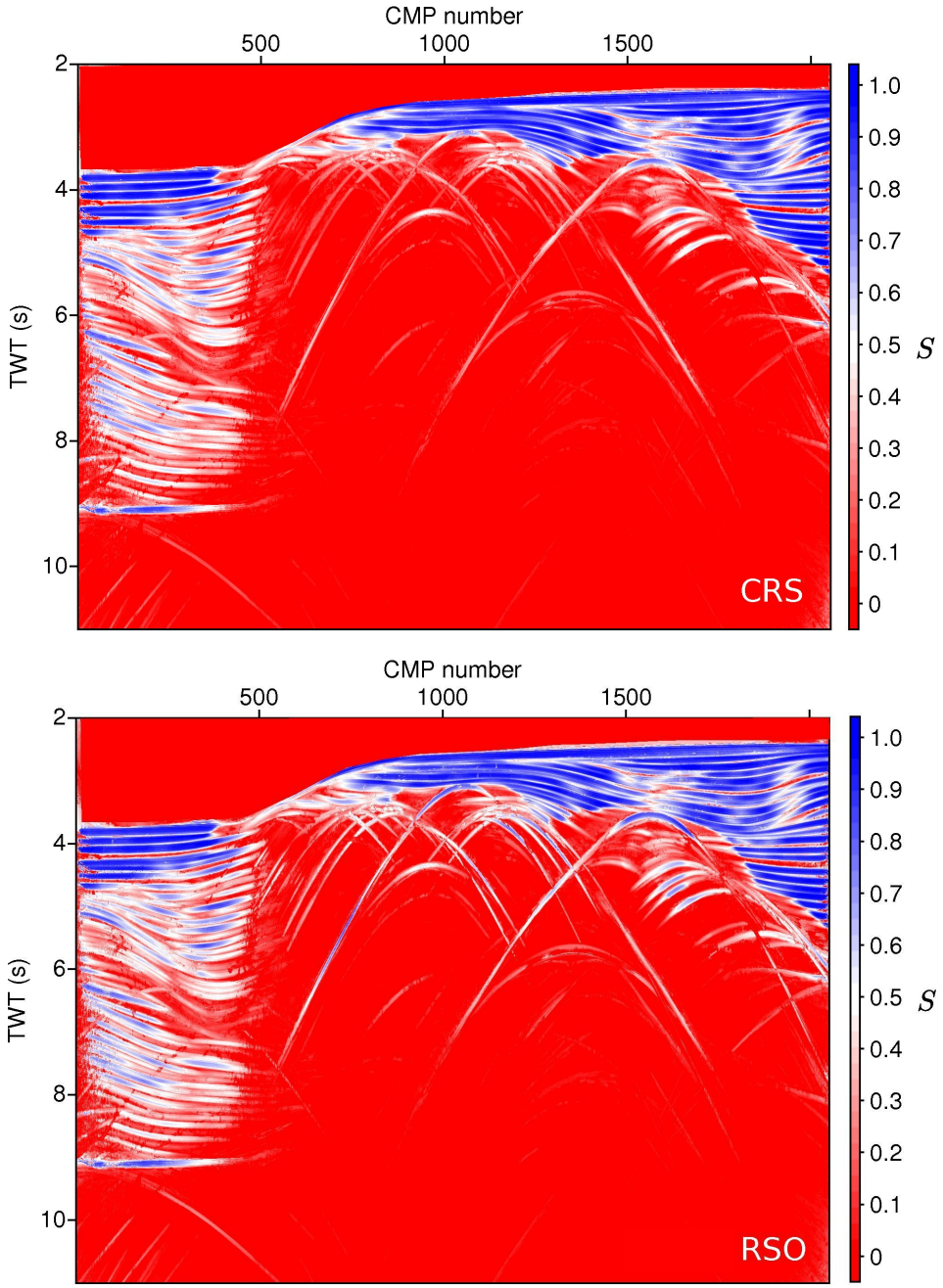

Figure 5: CRS and RSO semblance sections for the Sigsbee 2a dataset. Overall, the events stemming from features with low curvature are sufficiently well described by the CRS operator. RSO is equally well capable of approximating reflection events that are connected with nearly horizontally stratified layers. Especially the diffraction patterns related to the rugged top-of-salt are substantially better described by the double-square-root-based recursive stacking operator.

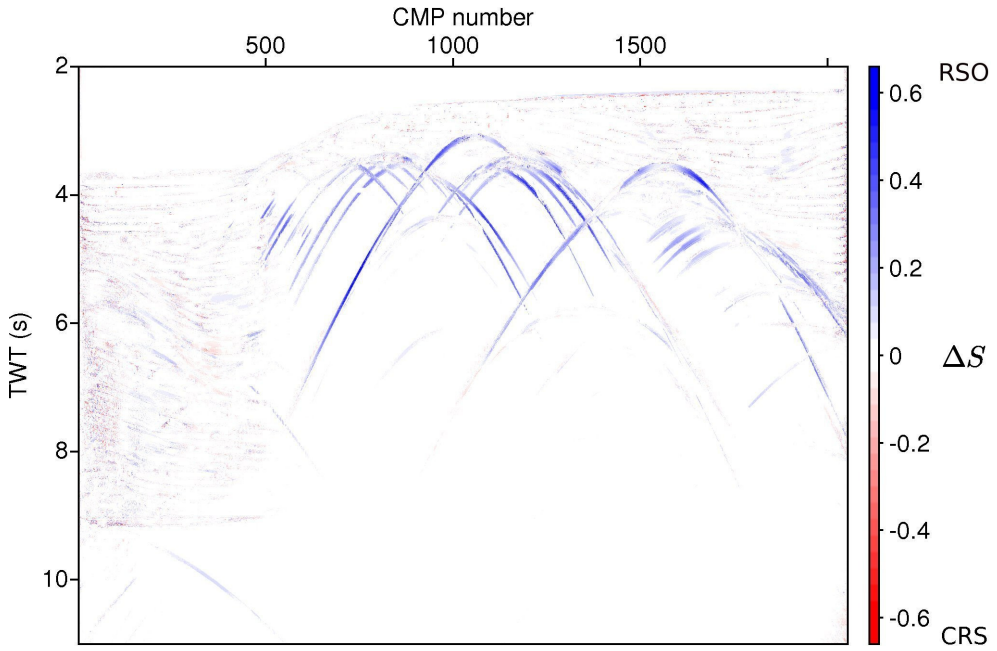

Figure 6: Difference in semblance between CRS and RSO. Diffraction events are much better described by the recursive approach, resulting in differences in semblance of up to ~ 0.6.

portions it appears as a continuous feature in the RSO counterpart, which is in good consistency with the depth model.

Although the superior performance of the poststack time migration algorithm can, in principle, as well be caused by the higher quality of the stacked section (due to a better fit to events in the data), comparison of Figures 11 and 12, where the ratio R_{NIP}/R_N is displayed, clearly reveals that RSO provides more reasonable attribute estimates for the diffraction events. This ratio should be equal to 1 for events stemming from point-like structures. For all main diffractions connected with the top-of-salt, the RSO estimates' ratio shows values closer to 1 than its CRS counterpart.

CONCLUSIONS AND OUTLOOK

We have applied the recursive stacking operator (Vanelle et al., 2010), parameterized in terms of the CRS attributes, to synthetic datasets with underlying models of different complexity. For the case of a spherical reflector in a constant vertical velocity gradient medium the Taylor-series-expansion-based RSO parameterization not only provided the highest semblance values, i.e. the best fit to the prestack data, but also the most reliable attribute estimates for all interface curvatures. In contrast to this parameterization, the shifted RSO expression as well as planar multifocusing turned out to be noticeably affected by the strength of the velocity gradient in the overburden. Confirming the results of Schwarz et al. (2011), where the pure traveltime fit was investigated, both operators led to the same values of semblance for the full range of curvatures for all considered gradients. In contrast to the double-square-root-based descriptions and in consistency with Schwarz et al. (2011), CRS fits events noticeably worse when they stem from highly-curved structures in the subsurface, resulting in lower semblance values and higher deviations of the attribute estimates. CRS turned out to systematically underestimate the emergence angle and the NIP-wave radius and overestimate the radius of the normal wave for high curvatures. The RSO parameterization based on the Taylor series expansion provided consistently accurate estimates over the full curvature range.

For the complex Sigsbee 2a model, the Taylor-series-expansion-based RSO expression is significantly more accurate than CRS in describing diffraction events in the prestack data. Its performance is comparable to the one of CRS for low reflector curvatures, which is in perfect agreement with the results gained for the spherical reflector model. The superior fit of diffractions not only results in an improved stack but

also in more reliable estimates of the kinematic wavefield attributes for these events, which clearly affects subsequent processing steps like the considered approximate poststack time migration. This confirms the result from the gradient medium.

Future work on the practical side includes the application of RSO to more complex models. Furthermore, the promising synthetic data results need to be confirmed for field data. Another future aspect is the performance of RSO for the separation of diffraction and reflection events. The extension of the method to three dimensions is straight forward, but has not been implemented yet. Furthermore, a modified RSO description capable to account for anisotropy (Vanelle et al., 2011) and converted waves is currently investigated.

ACKNOWLEDGEMENTS

We thank the members of the Applied Seismics Group Hamburg for continuous and fruitful discussions. This work was kindly supported by the sponsors of the Wave Inversion Technology Consortium. Seismic Un*x routines were used to create the spherical reflector datasets. The Sigsbee 2a synthetic seismic data were produced by the Subsalt Multiples Attenuation and Reduction Technology Joint Venture (SMAART JV).

REFERENCES

Mann, J. (2002). *Extensions and Applications of the Common-Reflection-Surface Stack Method*. PhD thesis, Universität Karlsruhe.

Müller, T. (1999). *The Common Reflection Surface stack method – Seismic imaging without explicit knowledge of the velocity model*. PhD thesis, Universität Karlsruhe.

Schwarz, B. (2011). A new nonhyperbolic multi-parameter stacking operator. Master's thesis, Universität Hamburg.

Schwarz, B., Vanelle, C., and Gajewski, D. (2011). The recursive stacking operator (RSO) Part 1: From RSO to CRS parameters. *15th Annual WIT report*.

Vanelle, C. (2002). *Traveltime-Based True-Amplitude Migration*. PhD thesis, Universität Hamburg.

Vanelle, C., Bobsin, M., Schemmert, P., Kashtan, B., and Gajewski, D. (2011). RSO: a new multiparameter stacking operator for an/isotropic media. *15th Annual WIT report*.

Vanelle, C., Kashtan, B., Dell, S., and Gajewski, D. (2010). A new stacking operator for curved subsurface structures. *SEG, Expanded Abstracts*, 29:3609–3613.

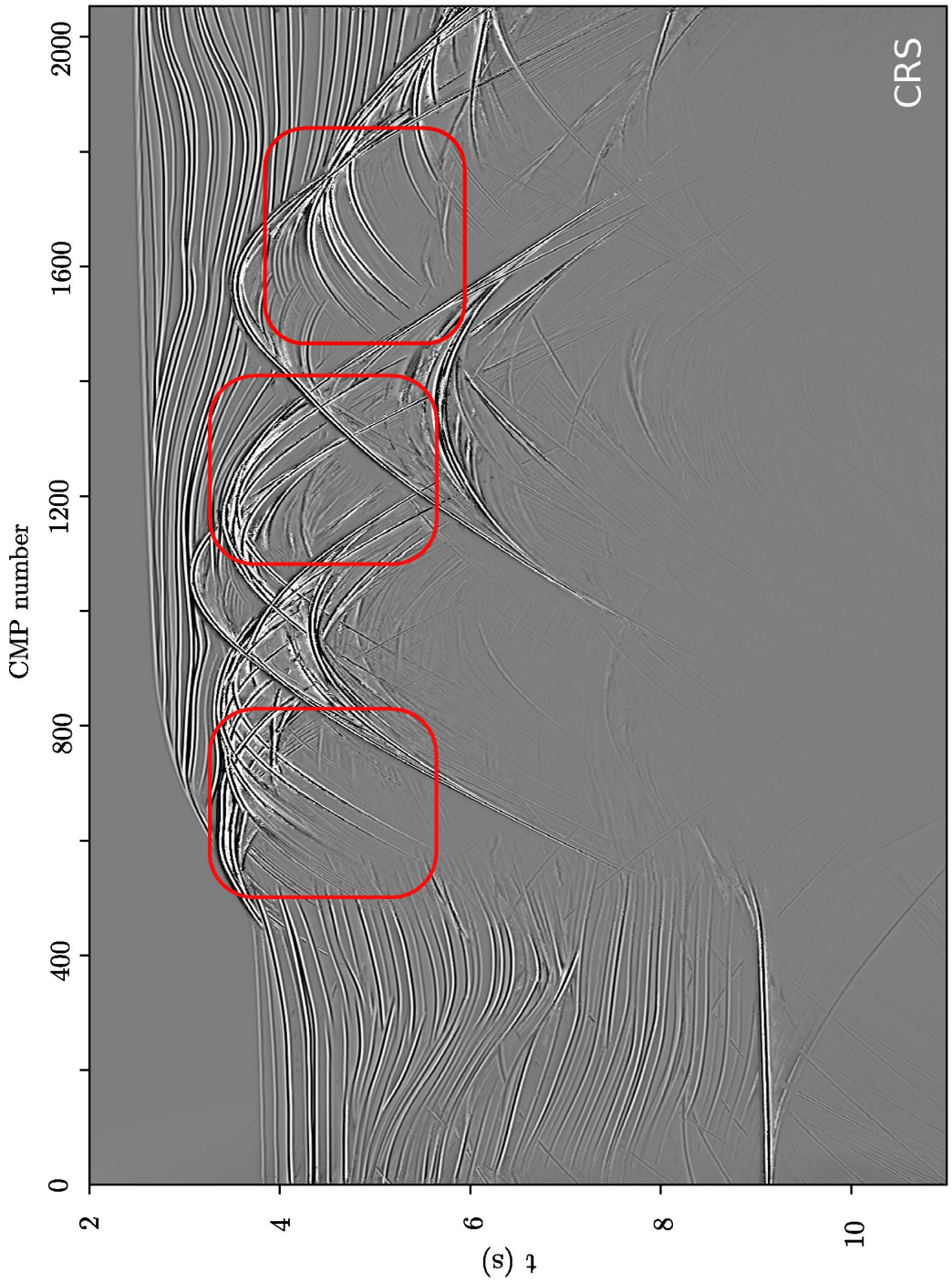

Figure 7: CRS-stacked section of the Sigsbee 2a dataset. CRS provides a reliable simulated zero-offset section with a high signal-to-noise ratio. While the events stemming from nearly planar structures left and above the salt are very crisply imaged, especially diffractions show distortions in the stacked waveforms. The red boxes indicate the major and most eye-catching differences between the CRS and RSO stack section.

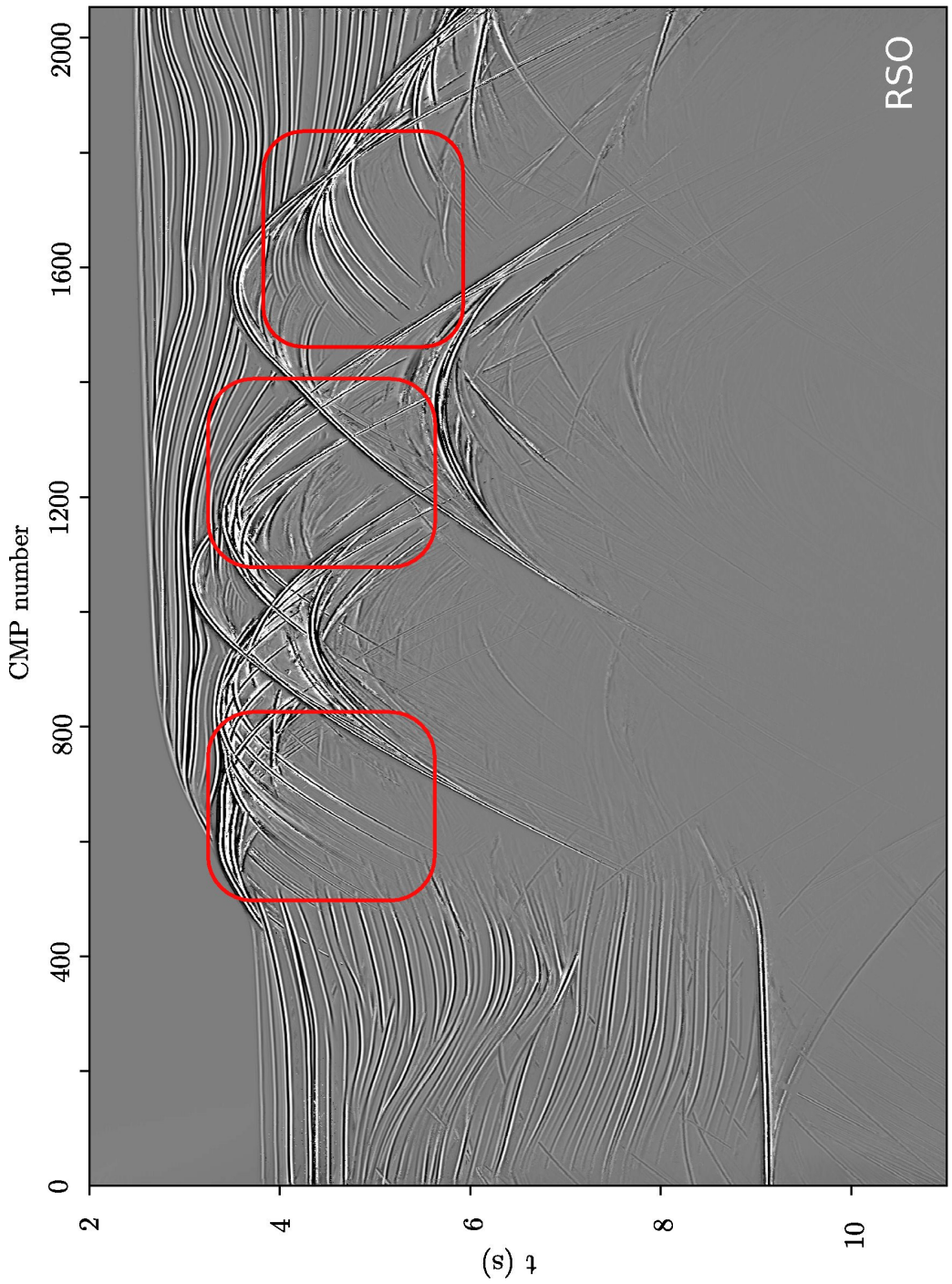

Figure 8: RSO-stacked section of the Sigsbee 2a dataset. Besides the comparably good quality of the image for events stemming from nearly planar features in the model, noticeable differences in amplitude and event continuity can be identified for the diffractions connected with the top-of-salt. The red boxes indicate the major improvements in the stack section, that result from the application of the recursive operator.

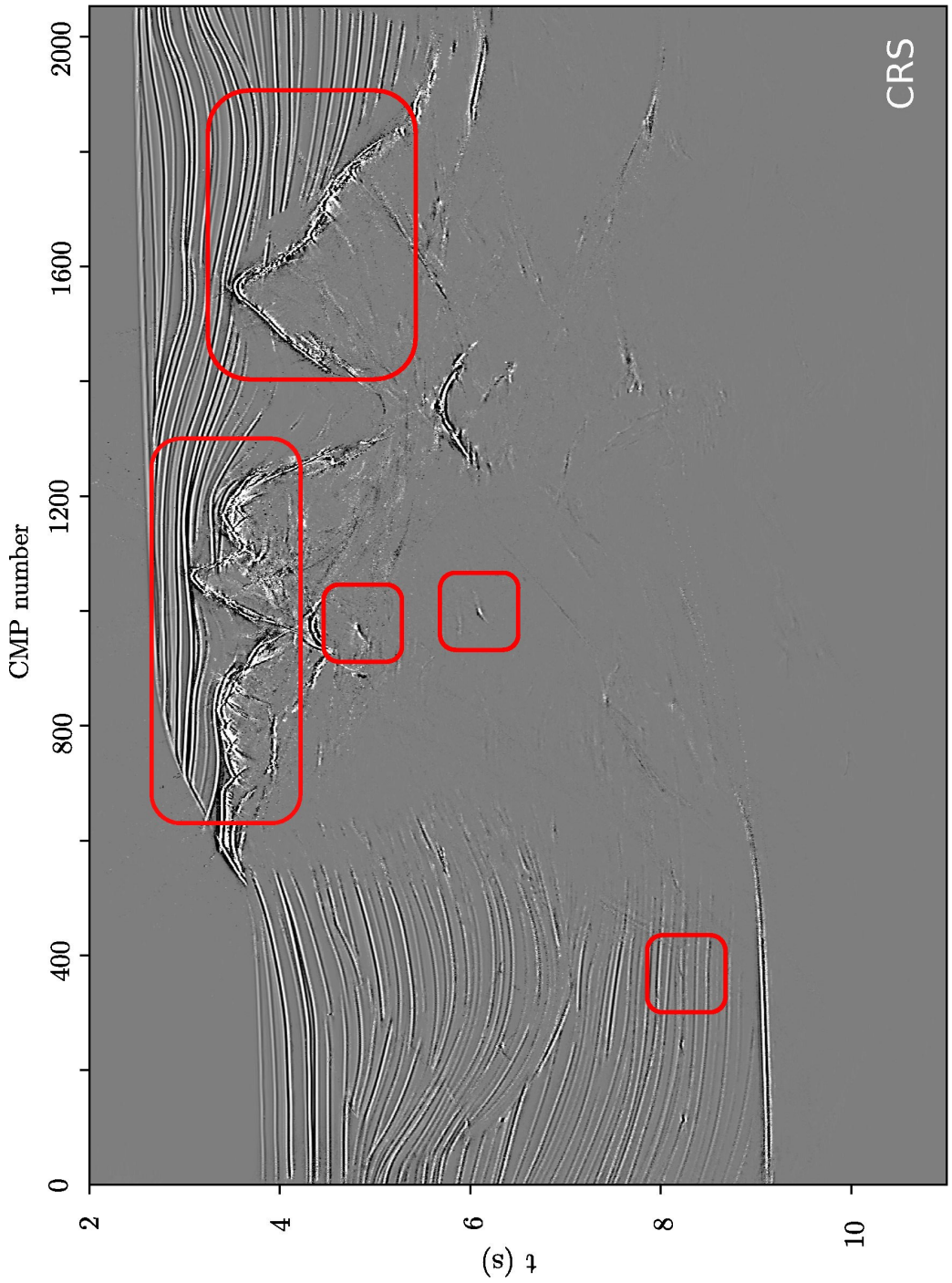

Figure 9: Time-migrated CRS-stacked section of the Sigsbee 2a dataset. Overall the approximate migration algorithm managed to collapse large portions of the scattered energy in the stack. However, most diffractions are not completely focused and residuals remain in the image. In consequence, the top-of-salt appears as a discontinuous feature. The red boxes indicate the major differences between the time migrated CRS and RSO stack section.

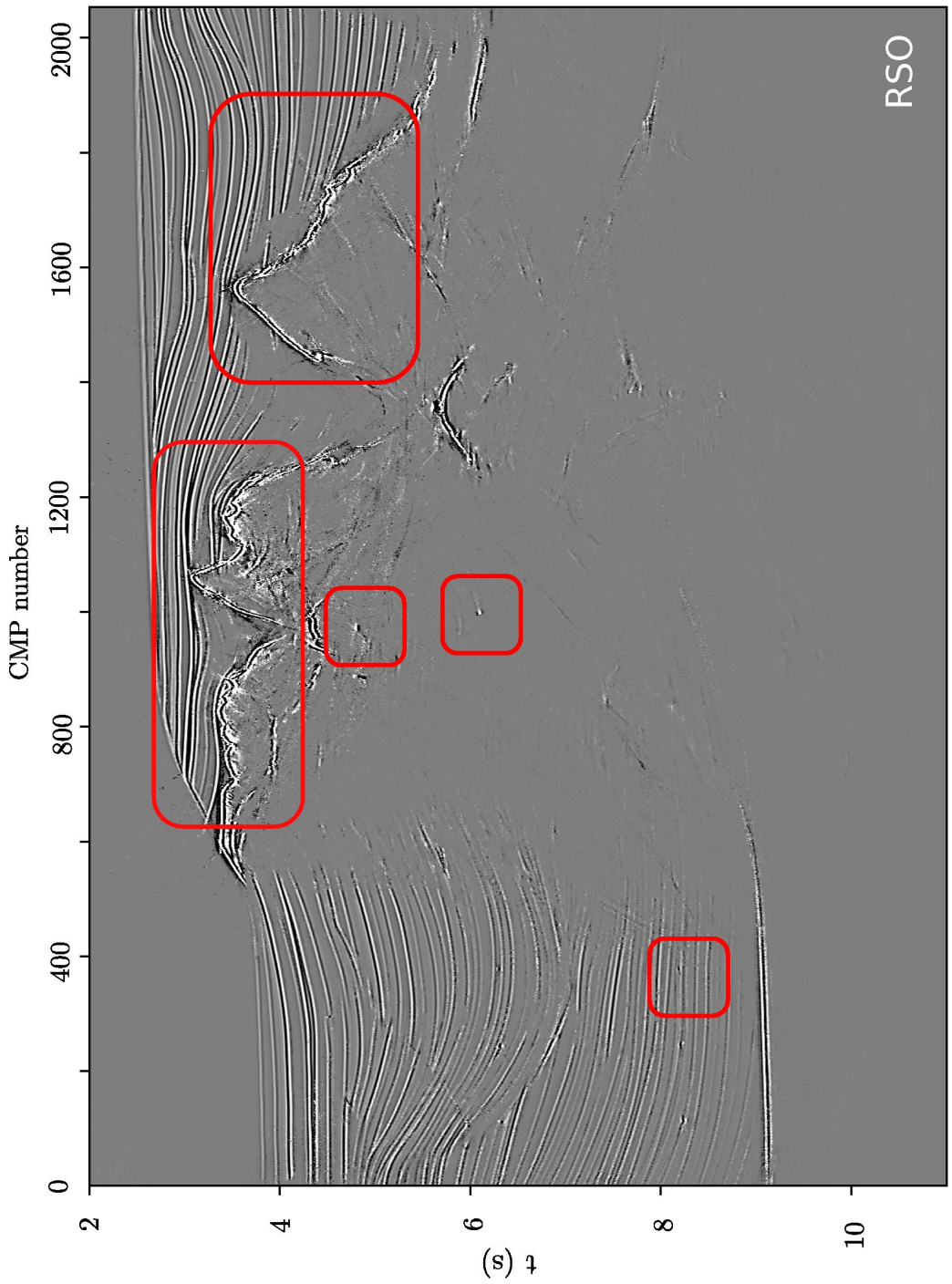

Figure 10: Time-migrated RSO-stacked section of the Sigsbee 2a dataset. While for CRS the migration algorithm fails to sufficiently collapse the diffraction events stemming from the rugged top-of-salt, application of RSO leads to a much cleaner subsequent migration result. The top-of-salt for the most part appears as a continuous feature, which is in good agreement with the depth model. Major improvements of the RSO time migrated stack section over the one of CRS are indicated by the red boxes.

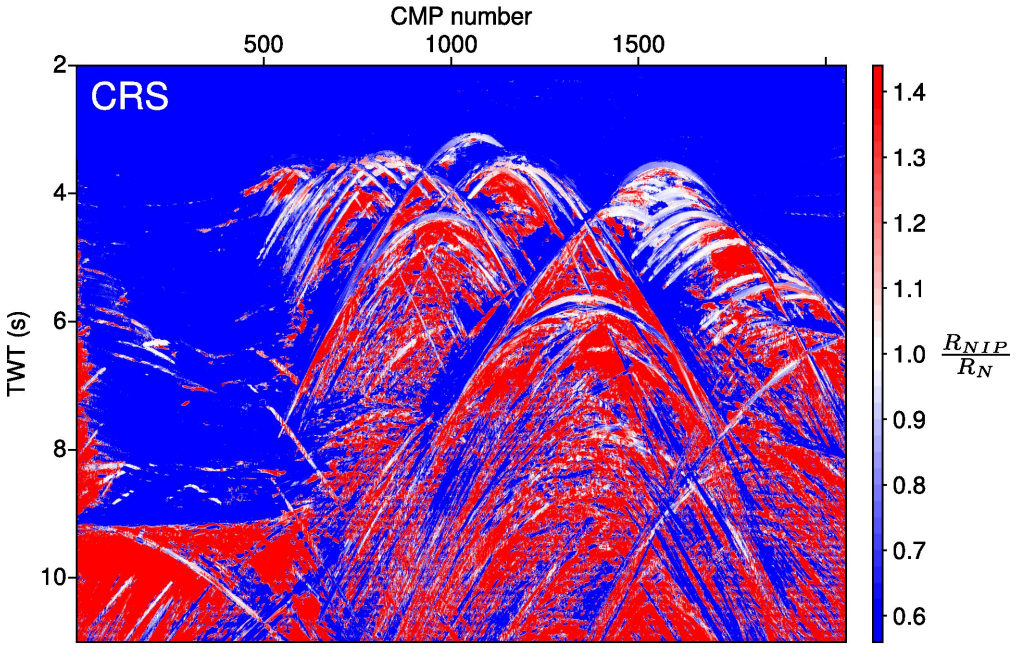

Figure 11: R_{NIP}/R_N section for the respective estimates of the CRS operator. Although overall providing a proper indication of the diffracted events in the data, the quality of the estimates appears to decrease for larger displacements from the apex.

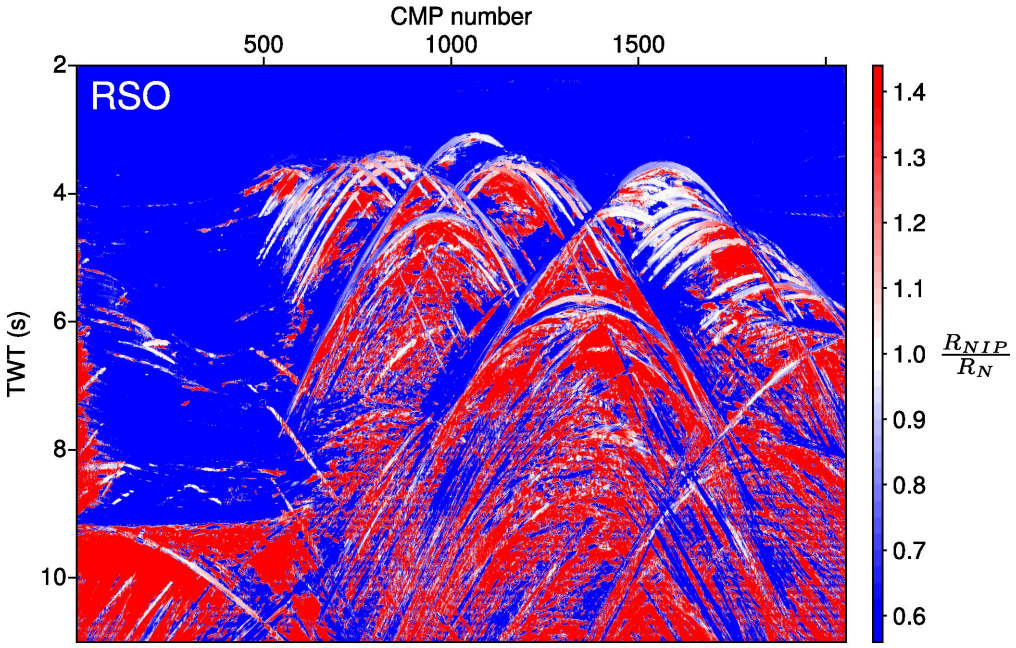

Figure 12: R_{NIP}/R_N section for the estimates of the recursive operator. Especially for higher lateral displacements from the diffractions' apices, the RSO estimates more clearly indicate the diffracting nature of the structures that cause the respective events.